

RESEARCH

Open Access



Aberrant expression of NEDD4L disrupts mitochondrial homeostasis by downregulating CaMKK β in diabetic kidney disease

Fei Han^{1†}, Shi Wu^{1†}, Ya Dong¹, Yanjie Liu¹, Bei Sun¹ and Liming Chen^{1*}

Abstract

Disturbance in mitochondrial homeostasis within proximal tubules is a critical characteristic associated with diabetic kidney disease (DKD). CaMKK β /AMPK signaling plays an important role in regulating mitochondrial homeostasis. Despite the downregulation of CaMKK β in DKD pathology, the underlying mechanism remains elusive. The expression of NEDD4L, which is primarily localized to renal proximal tubules, is significantly upregulated in the renal tubules of mice with DKD. Coimmunoprecipitation (Co-IP) assays revealed a physical interaction between NEDD4L and CaMKK β . Moreover, deletion of NEDD4L under high glucose conditions prevented rapid CaMKK β protein degradation. In vitro studies revealed that the aberrant expression of NEDD4L negatively influences the protein stability of CaMKK β . This study also explored the role of NEDD4L in DKD by using AAV-shNedd4L in db/db mice. These findings confirmed that NEDD4L inhibition leads to a decrease in urine protein excretion, tubulointerstitial fibrosis, and oxidative stress, and mitochondrial dysfunction. Further in vitro studies demonstrated that si-Nedd4L suppressed mitochondrial fission and reactive oxygen species (ROS) production, effects antagonized by si-CaMKK β . In summary, the findings provided herein provide strong evidence that dysregulated NEDD4L disturbs mitochondrial homeostasis by negatively modulating CaMKK β in the context of DKD. This evidence underscores the potential of therapeutic interventions targeting NEDD4L and CaMKK β to safeguard renal tubular function in the management of DKD.

Keywords Diabetic kidney disease, Mitochondrial homeostasis, NEDD4L, CaMKK β

[†]Fei Han and Shi Wu contributed equally to this work.

*Correspondence:

Liming Chen

xfx22081@vip.163.com

¹NHC Key Laboratory of Hormones and Development, Tianjin Key Laboratory of Metabolic Diseases, Chu Hsien-I Memorial Hospital Tianjin and Institute of Endocrinology, Tianjin Medical University, Tianjin 300134, China



© The Author(s) 2024. **Open Access** This article is licensed under a Creative Commons Attribution 4.0 International License, which permits use, sharing, adaptation, distribution and reproduction in any medium or format, as long as you give appropriate credit to the original author(s) and the source, provide a link to the Creative Commons licence, and indicate if changes were made. The images or other third party material in this article are included in the article's Creative Commons licence, unless indicated otherwise in a credit line to the material. If material is not included in the article's Creative Commons licence and your intended use is not permitted by statutory regulation or exceeds the permitted use, you will need to obtain permission directly from the copyright holder. To view a copy of this licence, visit <http://creativecommons.org/licenses/by/4.0/>. The Creative Commons Public Domain Dedication waiver (<http://creativecommons.org/publicdomain/zero/1.0/>) applies to the data made available in this article, unless otherwise stated in a credit line to the data.

Introduction

Diabetic kidney disease (DKD) is deemed to be the most prevalent and serious long-term complication of diabetes [1]. Its clinical symptoms include the onset of proteinuria, and a subsequent decrease in glomerular filtration that correlates with glomerulosclerosis [2]. The theory regarding the tubular aspect of DKD has gained prominence in the past decade, underscoring the critical role of proximal tubule dysfunction in the manifestation of albuminuria related to diabetic tubulopathy [3]. Proximal tubular cells are rich in mitochondria, which provide the energy required for tubular secretion and reabsorption [4, 5]. The wellness of mitochondria is vital for facilitating appropriate oxidative phosphorylation and ATP production. Notably, in DKD patients and corresponding mouse models, specific disruptions in mitochondrial homeostasis within proximal tubules have been identified [6, 7]. Hence, enhancing mitochondrial homeostasis in renal proximal tubular cells is likely a promising therapeutic and preventive measure for DKD.

Mitochondria are exceedingly dynamic organelles that constantly undergo fusion/fission and turnover through mitochondrial biogenesis and mitophagy [8]. Mitochondrial fusion reduces stress by joining partially damaged mitochondrial contents as a form of complementation, whereas fission is necessary to clear damaged mitochondria via the segregation of dysfunctional mitochondria [9]. However, excessive mitochondrial fission can lead to mitochondrial fragmentation, impair the electron transport chain and cause abnormal accumulation of mitochondrial ROS (mito-ROS). This accumulation of mito-ROS can contribute to mitochondrial dysfunction in DKD [10, 11].

Calcium ions (Ca^{2+}), which serve as essential and consistent second messengers, also support mitochondrial function [12]. It directly affects CaMKK β (calmodulin-dependent protein kinase β), a standard downstream molecule in Ca^{2+} signaling, with its activity dependent on Ca^{2+} concentration [13]. Furthermore, CaMKK β has the capacity to phosphorylate and stimulate 5' AMP-activated kinase (AMPK) [14], recognized for its vital role in regulating cell energy metabolism, responding to oxidative stress, and monitoring mitochondrial operations [15]. The CaMKK β /AMPK signaling pathway has proven to significantly regulate the mitochondrial stability of tubular epithelial cells [16]. Its activation counters DKD by modulating apoptosis and autophagy in endothelial cells and podocytes [17, 18]. Nevertheless, the complete impact of the CaMKK β /AMPK pathway on the regulation of diabetic tubular epithelial cells remains to be fully elucidated.

Previous studies have shown that the attenuation of CaMKK β could contribute to the pathogenesis of DKD [17, 18]. However, the precise underlying mechanism

remains unclear. NEDD4L, a ligase enriched in the kidney, pancreas, and prostate, is primarily expressed in renal tubular epithelial cells. Existing data indicate that NEDD4L is deeply involved in multiple calcium-related pathways [19, 20]. Furthermore, NEDD4L-depleted cells displayed a heightened mitochondrial membrane potential and maintained a mitochondrial fusion status in response to metabolic stress [21]. In light of these findings, we postulate that NEDD4L potentially modulates mitochondrial homeostasis by influencing CaMKK β activity in diabetic renal tubular epithelial cells.

In our recent study, we illustrated the potential role of NEDD4L in inducing mitochondrial dysfunction in diabetic proximal tubular epithelial cells. It was also established that the disruption of mitochondrial homeostasis in DKD could be attributed to the inhibition of CaMKK β /AMPK signaling. Interestingly, our results suggest that NEDD4L targets the degradation of CaMKK β , leading to the suppression of the CaMKK β /AMPK signaling pathway and subsequent mitochondrial impairment in proximal tubular epithelial cells.

Materials and methods

Animal models

Eight-week-old male db/db mice and their non-diabetic db/m littermates were obtained from Jicui Bioscience Co. Ltd. (Jiangsu, China), and were used as the type 2 diabetes models. All mice were housed individually, subjected to a 12-hour light/dark cycle, given free access to water, and were nourished with a standard laboratory diet. Twenty of the db/db mice were given injections of either adeno-associated virus (AAV)-shNedd4l-EGFP or the control virus (Yuanjing Biosciences, Guangdong, China). The Animal Care Committee of Tianjin Medical University strictly regulated all animal experiments according to its established guidelines and regulations.

Cell culture

Proximal tubular epithelial cells of human origin, HK-2, were procured from the Cell Bank of the Chinese Academy of Sciences, based in Shanghai, China, and subsequently cultured in DMEM medium, which was fortified with a 10% concentration of fetal bovine serum. The HK-2 cells were subjected to culture conditions that consisted of either a normal glucose concentration of 5.5 mM or a high glucose (HG) concentration of 25.5 mM over a period of 48 h. Additionally, 20.0 mM mannitol was used as an osmolality control. The cell transfection process was executed using the plasmids pcDNA3.1-CaMKK β (FulenGen, Guangdong, China), Nedd4L-siRNA (Ribobio, Guangdong, China) and CaMKK β -siRNA (Ribobio, Guangdong, China), along with the Lipofectamine 2000 reagent (Invitrogen, California, USA) in compliance with the guidelines provided by the manufacturer.

Renal histological analysis

As previously described [22], renal histological examination was conducted. Briefly, protocols provided by the manufacturer were followed to stain kidney sections with Hematoxylin and Eosin (HE), Masson's trichrome, and Periodic acid-Schiff (PAS). For immunohistochemical (IHC) analysis, kidney sections were blocked and incubated with primary antibodies. Subsequent incubation with secondary antibodies was performed before visualization using diaminobenzidine. The final step of counterstaining was performed with hematoxylin.

Western blotting analysis

Total proteins or mitochondrial proteins were isolated, separated and transferred onto polyvinylidene fluoride membranes (Millipore, Boston, USA). The membranes were incubated overnight with primary antibodies. The primary antibodies and their respective dilutions were NEDD4L, p-AMPK, AMPK, DRP-1, and HSP60 (all with a dilution ratio of 1:1000, Cell Signaling Technology, Danvers, USA), CaMKK β and MFN-2 (1:1000 dilution, Abcam, Cambridge, UK), and phospho-DRP1 (Ser616) (1:1000 dilution, Biorbyt, Cambridge, UK). Following this procedure, the sections were incubated with secondary anti-mouse/rabbit antibodies (Sungene Biotech, Tianjin, China). The protein bands were subsequently visualized using ECL Blotting Detection Reagents (Invigentech, California, USA). The final quantification of these blots was achieved using densitometry via the application of ImageJ software.

Isolation of mitochondrial protein

The mitochondrial fractions were extracted with a Mitochondria/Cytosol Fractionation Kit (KeyGEN Bio-TECH, Jiangsu, China) according to the manufacturer's instructions.

Immunofluorescence (IF) staining

For IF staining of cells and tissues, the protocols used were identical to those used for IHC analysis. Following incubation with the primary antibody, the slides were subjected to serial incubation with goat anti-rabbit IgG/FITC at a concentration of 1:100 (Proteintech, Chicago, USA). Subsequently, the slides were imaged using an automated Leica DMI 4000 B inverted microscope equipped with a Leica DFC300 FX camera.

Assessment of mitochondrial morphology

After several treatments, the viable cells were incubated with MitoTracker (Cell Signaling Technology, Danvers, USA) following the manufacturer's guidelines. Subsequently, these cells were inspected via confocal microscopy.

Albumin uptake analyses

The endocytosis assay was conducted according to a previously established procedure. In brief, HK2 cells were washed with warm Hanks' balanced salt solution (without phenol red) and subsequently incubated with 0.5 mg/ml TRITC-bovine serum albumin (BSA) (Sigma-Aldrich, USA) for one-quarter of an hour at 37 °C. After incubation, six washes were performed on the cells using cold Hanks' balanced salt solution (at 4 °C), followed by lysis in PBS buffer. A confocal fluorescence microscope (Leica Microsystems, Germany) was used to detect the fluorescence within the lysate.

Detection of ROS

To assess intracellular and mitochondrial ROS production, cells were incubated with H2DCFDA (Keygenbio, China) or MitoSOX (Keygenbio, China), respectively, and examined by microscopy. Intracellular ROS production in kidney tissues was evaluated utilizing 4-mm-thick cryostat sections, which were then stained with dihydroethidium (DHE) acquired from EVERBRIGHT, USA.

Co-immunoprecipitation (Co-IP)

The immunoprecipitation (IP) experiments were conducted in accordance with the methods previously reported [23]. Briefly, cells were harvested and lysed in IP lysis buffer, which consisted of 50 mM Tris (pH 7.4), 1 mM EDTA, 150 mM NaCl, 0.5% NP-40, and 1 \times protease inhibitor cocktail. Following an incubation period of one hour at 4 °C, the cell lysates were centrifuged at 14,000 \times g for 10 min at 4 °C. Both NEDD4L and CaMKK β were immunoprecipitated from 500 mg of the digitonin-solubilized proteins using Protein A/G PLUS-Agarose (Santa Cruz Biotechnology, CA, USA) according to the manufacturer's guidelines. The immunocaptured proteins were then subjected to SDS-PAGE/immunoblotting to analyze protein-protein interactions.

Statistical analyses

SPSS 19.0 software was used for statistical analysis. All the values are expressed as the mean \pm SEMs. The data were analyzed using one-way analysis of variance (ANOVA) or the least significant difference (LSD) test. A value of $P < 0.05$ was considered to indicate statistical significance.

Results

Alterations in mitochondrial dynamics in renal proximal tubular cells of diabetic mice

We conducted an immunostaining examination with DHE to investigate ROS production in the kidneys. As illustrated in Fig. 1A, ROS production was significantly greater in the kidneys of diabetic mice than in those of normal control mice. Additionally, the SOD2

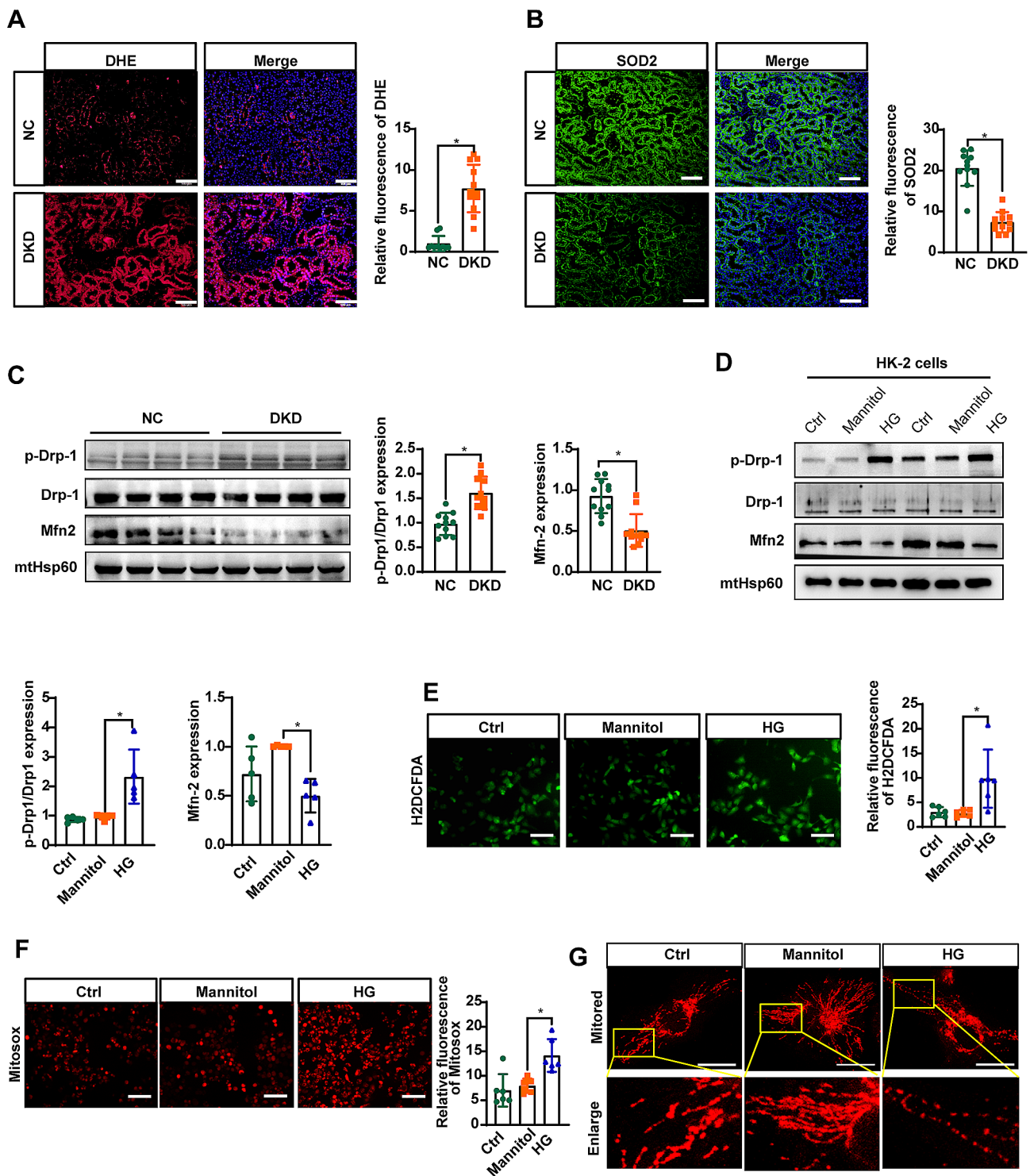


Fig. 1 Imbalanced mitochondrial homeostasis is associated with renal proximal tubular injury in DKD. **A** DHE staining was performed to evaluate the production of ROS in the kidneys of the mice. **B** Representative images of SOD2 staining of kidneys from mice. **C** and **D** Representative immunoreactive bands for Drp1, phosphorylated Drp1, Mfn2, and HSP60 in the mitochondrial fractions of the mice (**C**) and HK-2 cells (**D**) as indicated. **E** and **F** H2DCFDA (**E**) and Mitosox (**F**) staining were performed to evaluate the generation of ROS in the cytoplasm and mitochondria of HK-2 cells, respectively. **G** Representative images of MitoTracker Red-stained cells showing mitochondrial morphology in the indicated groups of cells. Scale bar = 100 μ m in A and B for fluorescence images, 50 μ m for images in E and F, and 20 μ m for confocal images in G. For all statistical plots, the data are presented as the means \pm SEMs. * $P < 0.05$

immunostaining level in diabetic mice was markedly lower than that in normal control mice, as indicated in Fig. 1B. Previous studies have highlighted the presence of excessive mitochondrial fission and fragmentation during the progression of DKD [24, 25]. Immunoblotting of isolated mitochondria revealed increased levels of phosphorylated Drp1 and decreased levels of Mfn-2 in diabetic mice compared with those in normal controls (Fig. 1D). These protein trends in HK-2 cells cultured with HG align with the findings in diabetic mice. Notably, HG treatment significantly promoted cytosolic and mitochondrial ROS generation in HK-2 cells, as demonstrated by H2DCFDA and Mitosox staining in (Fig. 1E, F). Furthermore, a reduction in mitochondrial length was observed in HK-2 cells exposed to HG conditions for 48 h (Fig. 1G).

CaMKK β -mediated protective effect on tubular injury in DKD

The IHC analysis uncovered that CaMKK β expression was predominantly localized in the renal proximal tubules. Notably, this expression was markedly diminished in the renal tubules of diabetic mice (Fig. 2A). This study also confirmed the decrease in CaMKK β protein in DKD mice and HG-treated HK-2 cells (Fig. 2B-D). In addition, the expression of p-AMPK/AMPK was significantly decreased under diabetic conditions (Fig. 2B, C). The function of CaMKK β in HG-induced HK-2 cells was explored in cells transfected with CaMKK β -overexpressing plasmids, resulting in a notable augmentation of p-AMPK/AMPK expression (Fig. 2E). Additionally, BSA-TRITC uptake in HK-2 cells significantly increased following CaMKK β overexpression (Fig. 2F). H2DCFDA and Mitosox staining indicated that the overexpression of CaMKK β suppressed ROS generation (Fig. 2G). Overexpression of CaMKK β also improved mitochondrial defects by increasing the mitochondrial length and density in HK-2 cells (Fig. 2H). Notably, CaMKK β overexpression led to a decrease in Drp1 phosphorylation but an increase in Mfn-2 expression (Fig. 2I).

CaMKK β and NEDD4L interact directly

Our results and previous research showed that the expression of CaMKK β is downregulated in DKD [17, 18], however, the specific underlying mechanism remains elusive. The NEDD4 family is characterized by a unique modular domain architecture that contains an amino terminal Ca²⁺ phospholipid binding (C2) domain [26]. NEDD4L is one of the NEDD4 members, and is enriched in the kidney, primarily expressed in renal tubular epithelial cells. NEDD4L has a domain structure with a C2 domain at the N terminus, which can bind calcium [19], and functions as a ligase that facilitates the regulatory processes and binding of diverse membrane proteins for

their efficient internalization and turnover. Existing data indicate that NEDD4L is deeply involved in multiple calcium-related pathways [19, 20]. Moreover, depletion of NEDD4L in cells has been associated with heightened mitochondrial membrane potential and the maintenance of mitochondrial fusion status under metabolic stress [21]. In light of these findings, we propose that NEDD4L may modulate mitochondrial homeostasis by influencing CaMKK β in diabetic renal tubular epithelial cells. To investigate this hypothesis, we initially assessed the expression of NEDD4L in DKD mice through IHC, revealing a prominent localization of NEDD4L in renal proximal tubule cells, with a marked increase in diabetic mice (Fig. 3A), further validated by Western blotting (Fig. 3B). NEDD4L antibodies were used to isolate protein complexes from HK-2 cells, and these complexes were subsequently blotted with CaMKK β antibodies. As shown in Fig. 3C and D, a physical interaction between NEDD4L and CaMKK β was detected. In addition, double staining demonstrated a high level of co-localization of NEDD4L with CaMKK β (Fig. 3E).

Inhibition of NEDD4L ameliorates protein excretion in diabetic mice

db/db mice injected with AAV were used to investigate the involvement of NEDD4L in DKD development. Following injection of AAV-shNedd4L, the expression of NEDD4L in the renal cortex of db/db mice significantly decreased (Fig. 4A). Body weight and blood glucose levels did not significantly change across all groups (Fig. 4B, C). Protein excretion was significantly decreased in db/db mice injected with AAV-shNedd4L (Fig. 4D, E). Additionally, NAG and NAG/Cr also showed a decreasing trend, but the difference was not statistically significant (Fig. 4F, G). Previous studies have indicated that NEDD4L may impact the balance of potassium and sodium in the kidney [27, 28]. Furthermore, an analysis of potassium, sodium, and other ions in both blood and urine samples revealed no significant variations among the groups, as presented in Supplementary Fig. 1.

Inhibition of NEDD4L improves mitochondrial homeostasis in diabetic mice

The db/db mice injected with the negative control exhibited significant glomerular enlargement, mesangial matrix expansion, tubular hypertrophy, dilation, and disruption of the tubular basement membrane. Masson staining further revealed a notable increase in tubulointerstitial fibrosis in diabetic mice (Fig. 5A, B). However, diabetic mice injected with AAV-shNedd4L showed significant improvements compared to those in the negative control group (Fig. 5A, B). DHE staining demonstrated that AAV-shNedd4L alleviated oxidative stress in diabetic mice (Fig. 5C). Compared to the negative control

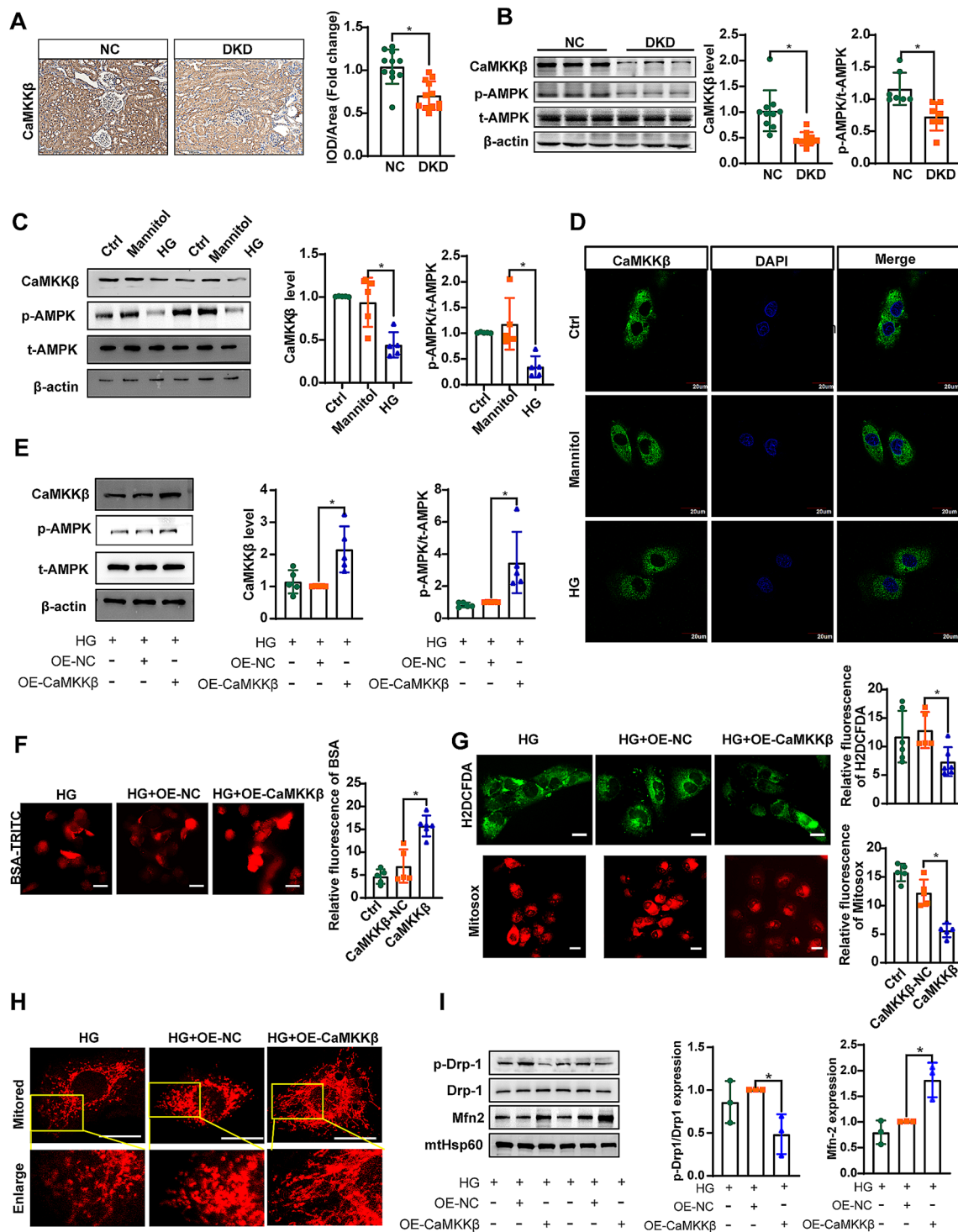


Fig. 2 CaMKKβ-mediated protective effect on tubular injury in DKD. **A** IHC staining was performed to evaluate the protein expression of CaMKKβ in kidneys of the mice. Scale bar = 200 μm. **B** and **C** Representative immunoreactive bands for CaMKKβ, AMPK, and phosphorylated AMPK in the groups of mice (**B**) and HK-2 cells (**C**) cultured with HG as indicated. **D** IF staining of CaMKKβ in HK-2 cells cultured with HG for 48 h. Scale bar = 20 μm. **E** Representative immunoreactive bands for CaMKKβ, AMPK, and phosphorylated AMPK in HK-2 cells transfected with CaMKKβ as indicated. **F** IF staining was performed to evaluate the uptake of BSA-TRITC in HK-2 cells. Scale bar = 50 μm. **G** H2DCFDA and Mitosox staining were performed to evaluate the generation of ROS in the cytoplasm and mitochondria of HK-2 cells, respectively. Scale bar = 20 μm. **H** Representative images of MitoTracker Red-stained cells showing mitochondrial morphology in the indicated groups of cells. **I** Representative immunoreactive bands for Drp1, phosphorylated Drp1, Mfn2, and HSP60 in the mitochondrial fraction of HK-2 cells transfected with CaMKKβ as indicated. Scale bar = 20 μm. OE-NC represents the control of CaMKKβ. OE-CaMKKβ represents the overexpression of CaMKKβ. For all the statistical plots, the data are presented as the means ± SEMs. **P* < 0.05

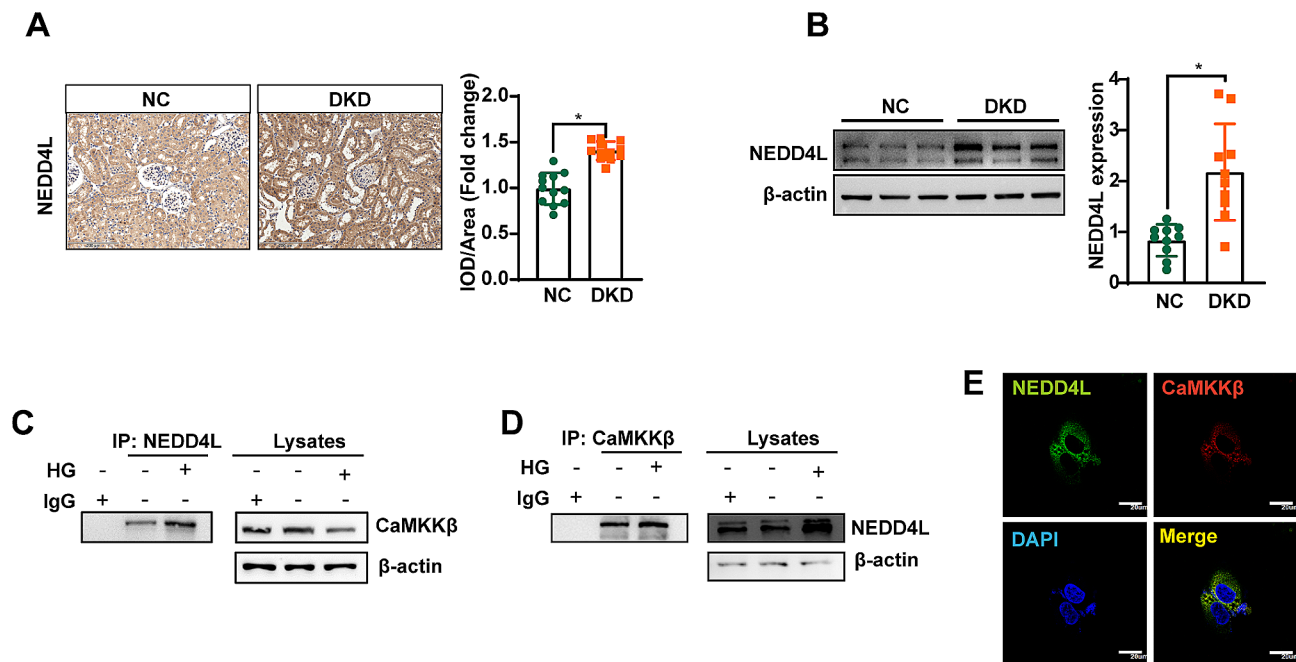


Fig. 3 NEDD4L physically interacts with CaMKK β . **A** IHC staining was performed to evaluate the protein expression of NEDD4L in the kidneys of mice. Scale bar = 200 μ m. **B** Representative immunoreactive bands for NEDD4L in groups of mice. For all statistical plots, the data are presented as the means \pm SEMs. * P < 0.05. **C** and **D** The interaction between NEDD4L and CaMKK β was detected in the Co-IP analysis of HK-2 cells. **E** Double staining showed co-localization of NEDD4L with the CaMKK β in HK-2 cells. Scale bar = 20 μ m

diabetic mice, shNedd4L-treated diabetic mice exhibited reduced renal apoptosis, as indicated by decreased expression of Bax/Bcl2 and cleaved Caspase3 (Fig. 5D). Additionally, CaMKK β /AMPK signaling was upregulated following shNedd4L treatment (Fig. 5E). Immunoblotting of isolated mitochondria revealed decreased phosphorylation levels of Drp1 and increased levels of Mfn-2 in the AAV-shNedd4L db/db mice as compared with the negative controls (Fig. 5F).

Silence of NEDD4L prevents HG-induced mitochondrial dysfunction in HK-2 cells

The uptake of BSA-TRITC in HG-treated HK-2 cells was significantly enhanced following the silencing of NEDD4L (Fig. 6A). Staining with H2DCFDA and Mito-sox revealed a marked suppression of ROS generation by si-Nedd4L (Fig. 6B). In vitro, si-Nedd4L improved mitochondrial defects, leading to increased mitochondrial length and density in HK-2 cells (Fig. 6C). Notably, si-Nedd4L significantly reduced the phosphorylation of Drp1 but increased Mfn-2 expression (Fig. 6D). Furthermore, transfection with si-Nedd4L rescued CaMKK β expression in HK-2 cells, as confirmed by Western blot analysis (Fig. 6E). The ratio of phosphorylated AMPK to total AMPK (p-AMPK/AMPK) was also notably elevated post NEDD4L knockdown (Fig. 6E).

NEDD4L leads to impaired mitochondrial homeostasis via CaMKK β expression inhibition

In HK-2 cells treated with HG, the expression of CaMKK β /AMPK pathway was upregulated by NEDD4L-siRNA, however, this upregulation was reversed by CaMKK β knockdown (Fig. 7A). Moreover, mitochondrial fission induced by HG was alleviated after NEDD4L knockdown, but this improvement was also abolished by CaMKK β knockdown (Fig. 7B, C). Additionally, CaMKK β -siRNA reversed the improvements in BSA uptake and oxidative stress observed following treatment with NEDD4L-siRNA (Fig. 7D-F). These results collectively suggest that NEDD4L may impact mitochondrial function through its regulation of the CaMKK β pathway.

NEDD4L negatively regulates the stability of CaMKK β

The expression of endogenous CaMKK β was significantly decreased under diabetic conditions (Fig. 2A-C). Furthermore, treatment with HG led to a time-dependent inhibition of CaMKK β expression (Fig. 8A). To further clarify whether HG affects CaMKK β stability through the proteasome or lysosome pathway, we treated cells with the proteasome inhibitor MG132 or the lysosome inhibitor chloroquine. The decrease in CaMKK β levels caused by HG could be effectively reversed by MG132 but not by chloroquine, suggesting that proteasome-mediated degradation is the primary cause of the HG-induced decrease in CaMKK β levels (Fig. 8B). Furthermore, the deletion of

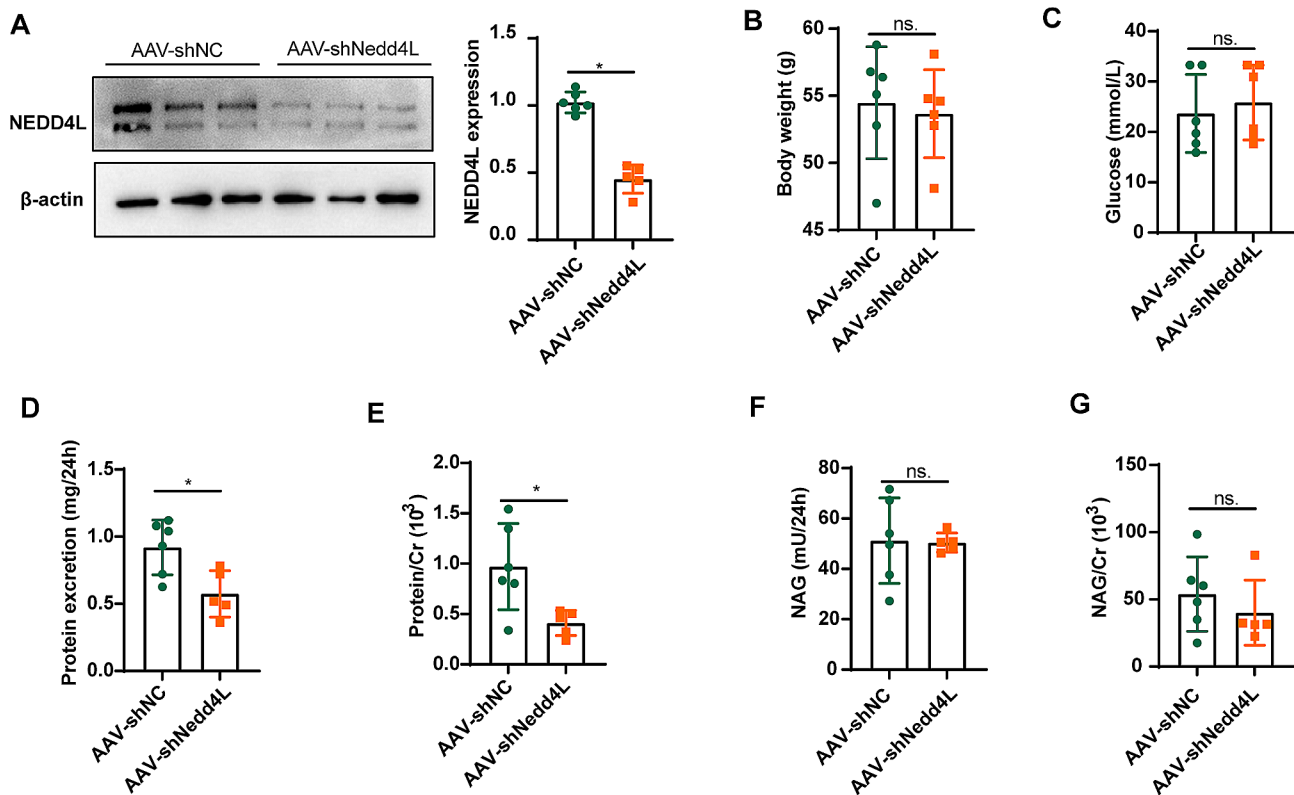


Fig. 4 Inhibition of NEDD4L ameliorates protein excretion in diabetic mice. Male db/db mice (8 weeks old) were fed a chow diet for 1 week and then injected with AAV-shNedd4L via the tail vein. **A** NEDD4L knockdown in the kidneys of db/db mice was confirmed by Western blot analysis. **B** and **C** Body weights (**B**) and fasting blood glucose (**C**) were measured in mice 8 weeks after viral infusion. **D** Twenty-four-hour urinary protein excretion was decreased in NEDD4L knockdown mice. **E-G** Protein/Cr (**E**), NAG (**F**), and NAG/Cr (**G**) in 24 h urine samples of the mice. For all the statistical plots, the data are presented as the means \pm SEMs. ns. indicates no significance; * $P < 0.05$

NEDD4L prevented the rapid decrease in CaMKK β protein levels after exposure to HG (Fig. 8C). Deletion of NEDD4L also reversed the decrease in total CaMKK β protein in HK-2 cells exposed to HG, which was not different from the effect of MG132 (Fig. 8D), indicating that Nedd4L-siRNA and MG132 inhibit different steps of the same CaMKK β degradation pathway under HG conditions. In summary, the presented findings provide substantial evidence that dysregulated NEDD4L disrupts mitochondrial homeostasis by adversely modulating CaMKK β in DKD (Fig. 8E).

Discussion

In this study, we found that increased NEDD4L expression in renal proximal tubules resulted in reduced BSA uptake, disrupted mitochondrial homeostasis, and elevated oxidative stress. Conversely, inhibition of NEDD4L effectively alleviated DKD. Our findings also revealed a significant association between the CaMKK β /AMPK pathway and mitochondrial function as well as apoptosis. Specifically, we observed a downregulation of the CaMKK β /AMPK pathway under diabetic conditions and demonstrated the protective role of CaMKK β

overexpression in HK-2 cells. Additionally, our study revealed that NEDD4L disrupts mitochondrial homeostasis by promoting the degradation of CaMKK β in DKD. These results suggest a potential mechanism by which NEDD4L contributes to renal proximal tubule dysfunction in DKD patients and highlight the importance of the CaMKK β /AMPK pathway in mitigating the effects of NEDD4L. Further exploration of these pathways may offer insights into novel therapeutic targets for DKD.

Ca²⁺ is an important and pervasive second messenger that also maintains the function of mitochondria [29]. CaMKK β /AMPK signaling plays an important role in regulating mitochondrial homeostasis. Prior research has demonstrated that A β 42 oligomers trigger mitochondrial fragmentation and synaptotoxicity through the overactivation of CaMKK β -AMPK [29]. CaMKK β /AMPK-mediated autophagy participates in podocyte injury under diabetic conditions [17, 18]. However, the role of the CaMKK β /AMPK pathway in regulating diabetic tubular epithelial cells remains unclear. Our data showed that the CaMKK β /AMPK pathway was suppressed in DKD, resulted in a reduction of mitochondrial fragmentation and oxidative stress, while enhancing the uptake of BSA

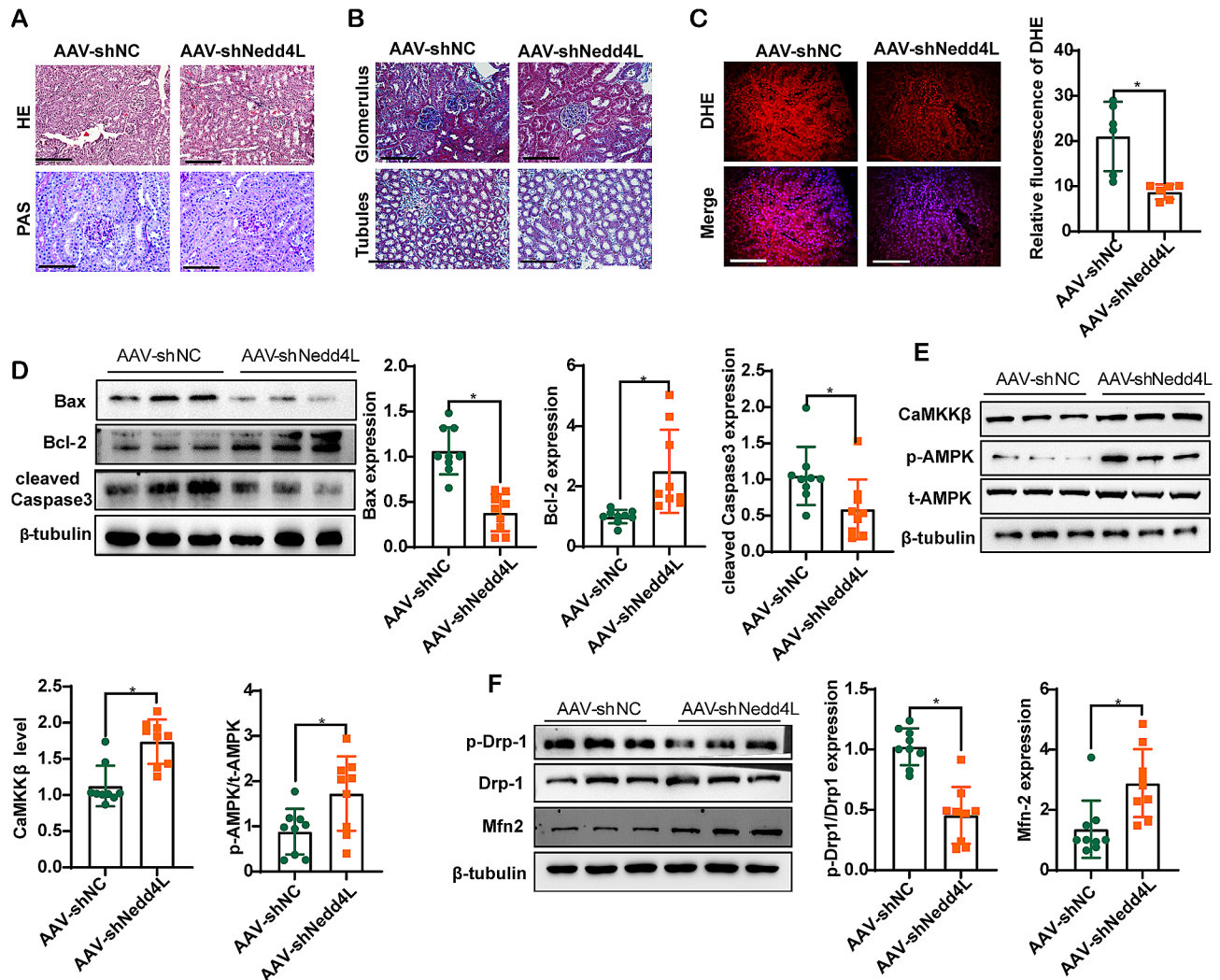


Fig. 5 Inhibition of NEDD4L ameliorates oxidative stress and mitochondrial dysfunction in diabetic mice. **A** Representative images of HE and PAS staining of kidney sections. **B** Representative images of Masson staining of kidney sections. **C** Representative images of DHE-stained kidney sections showing oxidative stress in the mice. A-C: Scale bar = 200 μ m. **D** Representative immunoreactive bands for Bax, Bcl-2, and cleaved Caspase-3 in the groups of mice. **E** Representative immunoreactive bands for CaMKK β , phosphorylated AMPK, and total AMPK in the groups of mice. **F** Representative immunoreactive bands for Drp1, phosphorylated Drp1, Mfn2, and HSP60 in different groups of mice, as indicated. For all the statistical plots, the data are presented as the means \pm SEMs. * P < 0.05

in HK-2 cells induced by HG. The above results demonstrated the protective role of CaMKK β /AMPK signaling in HK-2 cell function.

We sought to investigate the downregulation of CaMKK β under diabetic conditions and conducted MG-132 and chloroquine assays. Our findings indicate that proteasome-mediated degradation is the primary cause of HG-induced decreases in CaMKK β levels. The NEDD4 family members are characterized by a unique modular domain architecture containing an N-terminal C2 domain [26]. NEDD4L, a member of this family closely associated with Ca²⁺ signaling [30, 31], is involved in the regulation of protein stability [21, 32]. Our findings revealed a negative relationship between NEDD4L and CaMKK β levels. Deletion of NEDD4L prevented the

rapid degradation of the CaMKK β protein in response to HG exposure. Furthermore, in vitro studies indicated that abnormal expression of NEDD4L negatively regulates the protein stability of CaMKK β .

Our study revealed a significant elevation in the expression of NEDD4L specifically within the kidney, with a predominant localization in the renal proximal tubules. Utilizing AAV-shNedd4L for NEDD4L knockdown demonstrated a protective effect against DKD. A previous study showed that mice deficient in NEDD4L, specifically in the renal tubules (Nedd4L Ksp1.3), developed mild kidney disease due to the upregulation of ENaC [33]. Additionally, NEDD4L likely plays a role in maintaining the balance of potassium and sodium in the kidney [27, 28]. The aforementioned studies strengthened the

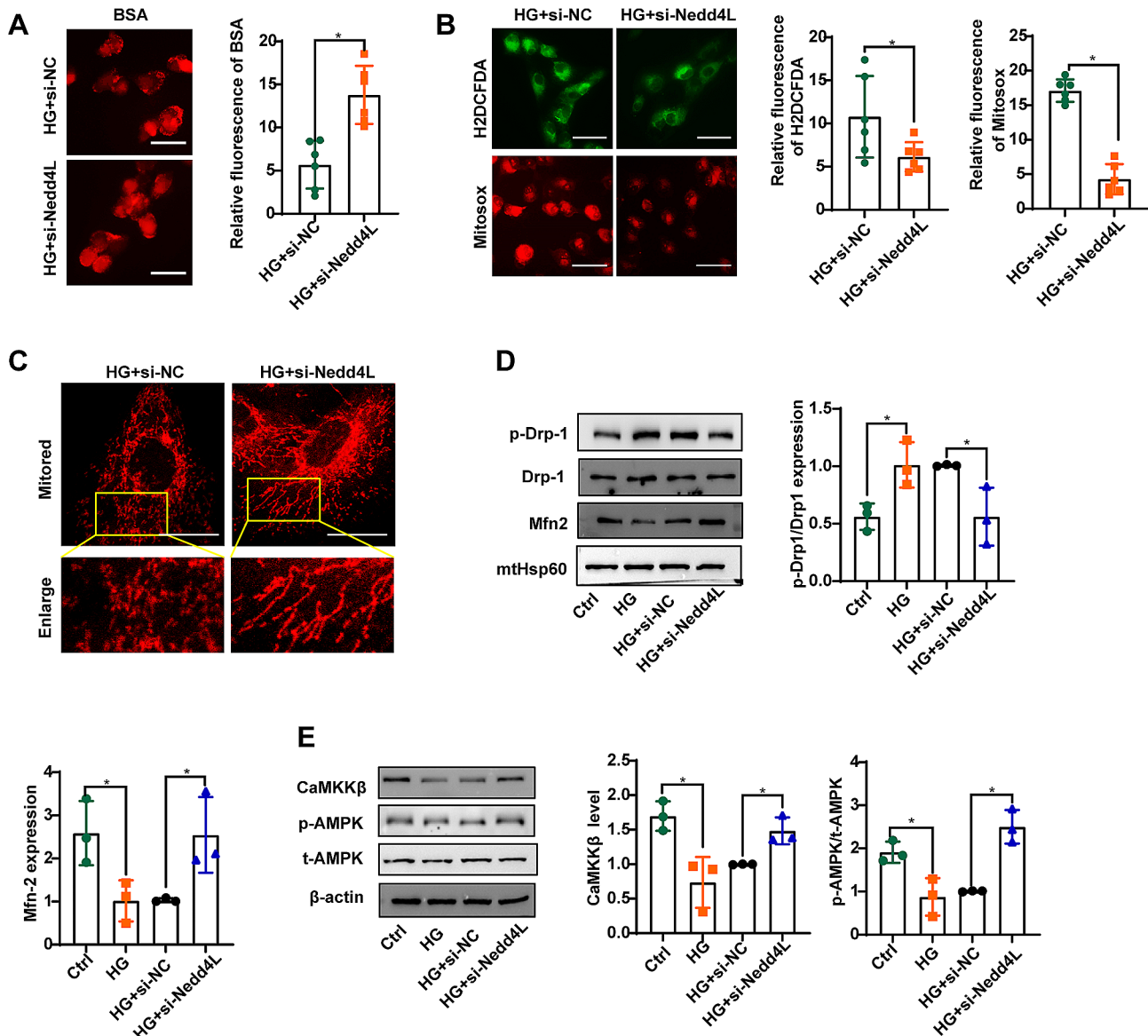


Fig. 6 Silencing NEDD4L prevents HG-induced mitochondrial dysfunction in HK-2 cells. **A** IF staining was performed to evaluate the uptake of BSA-TRITC in the experiments. **B** H2DCFDA and Mitosox staining were performed to evaluate the generation of ROS in the cytoplasm and mitochondria of HK-2 cells, respectively. Scale bar = 50 μ m. **C** Representative images of MitoTracker Red-stained cells showing mitochondrial morphology in the indicated groups of cells. Scale bar = 20 μ m. **D** Representative immunoreactive bands for Drp1, phosphorylated Drp1, Mfn2, and HSP60 in the mitochondrial fraction of HK-2 cells transfected with Nedd4L-siRNA as indicated. **E** Representative immunoreactive bands for CaMKK β , AMPK, and phosphorylated AMPK in HK-2 cells transfected with Nedd4L-siRNA as indicated. For all the statistical plots, the data are presented as the means \pm SEMs. * P < 0.05

understanding of the impact of NEDD4L on the kidney, primarily through its regulation of Na^+ and K^+ absorption. However, our current research demonstrated that knockdown of NEDD4L in the kidneys of db/db mice using AAV did not disrupt the balance of Na^+ and K^+ , potentially accounting for the discrepancies with previous findings. Nevertheless, further investigations are warranted to comprehensively elucidate the role of NEDD4L.

The role of mitochondrial integrity in kidney tubular cells is crucial for the efficient production of ATP and

oxidative phosphorylation. It has been suggested that enhancing the balance of mitochondria in renal proximal tubular cells could be a viable strategy for treating and preventing DKD. In our research, we investigated the influence of NEDD4L on mitochondrial dynamics and found that NEDD4L may contribute to mitochondrial fission, a finding that aligns with that of a previous study [21]. The aforementioned study demonstrated that cells with reduced NEDD4L exhibited elongated mitochondria in a more fused state than did control cells [21]. In our research, we observed that silencing NEDD4L attenuated

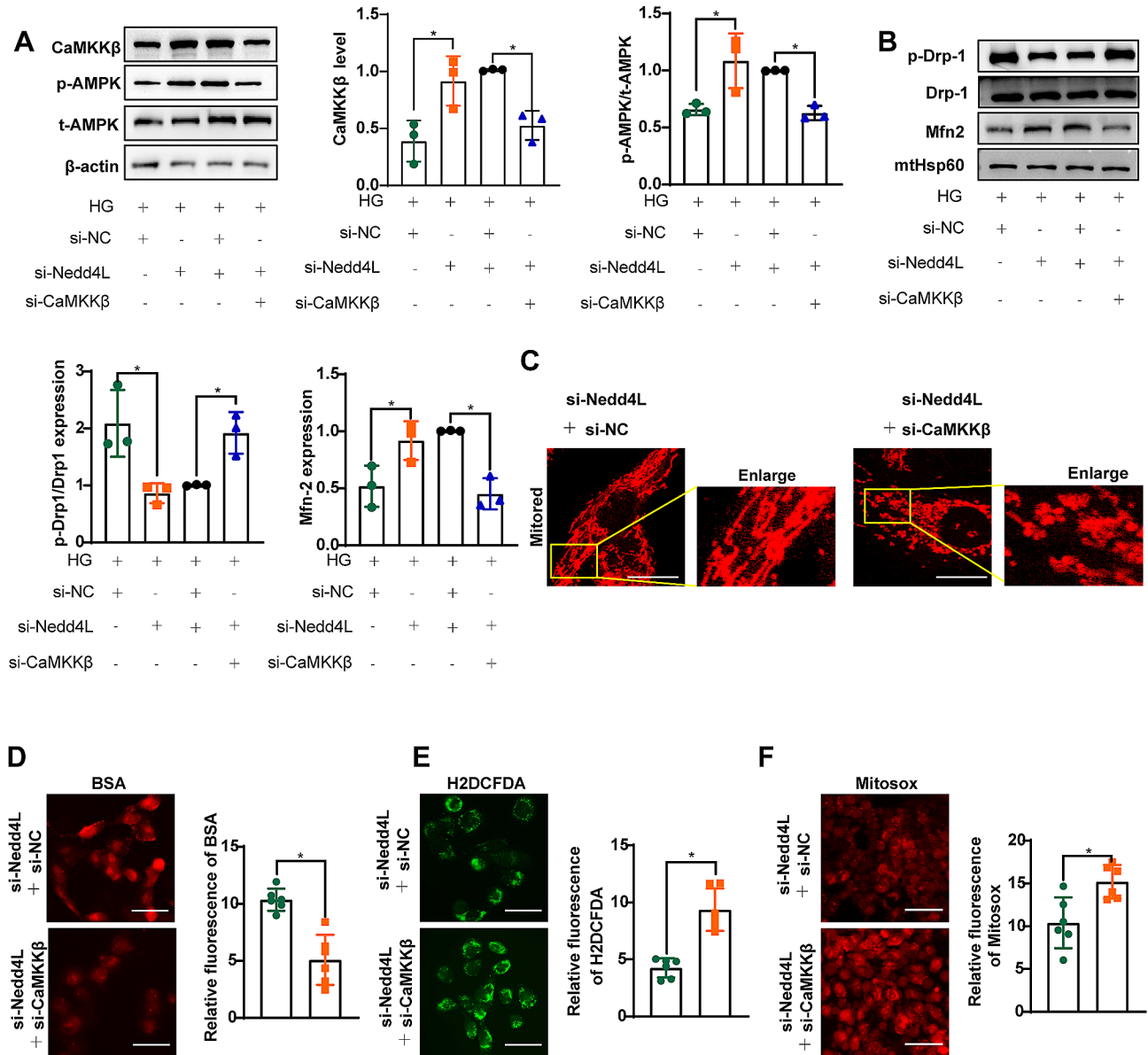


Fig. 7 Knockdown of NEDD4L contributes to HK-2 cell function via CaMKKβ/AMPK pathway. **A** Representative immunoreactive bands for CaMKKβ, AMPK, and phosphorylated AMPK in HK-2 cells cotransfected with Nedd4L-siRNA and CaMKKβ-siRNA as indicated. **B** Representative immunoreactive bands for Drp1, phosphorylated Drp1, Mfn2, and HSP60 in the mitochondrial fraction of HK-2 cells, as indicated. **C** MitoTracker Red staining showing mitochondrial morphology in the indicated groups of cells. Scale bar = 20 μm. **D** IF staining was performed to evaluate the uptake of BSA-TRITC in the indicated groups of cells. Scale bar = 50 μm. **E** and **F** H2DCFDA (E) and Mitosox (F) staining were performed to evaluate the generation of ROS in the cytoplasm and mitochondria of HK-2 cells, respectively. Scale bar = 50 μm. For all the statistical plots, the data are presented as the means ± SEMs. *P < 0.05

mitochondrial fission in HG-induced HK-2 cells. However, the effect of si-NEDD4L was nullified upon knockdown of CaMKKβ. These findings suggest that NEDD4L potentially influences DKD by modulating CaMKKβ and its downstream signaling pathways.

In conclusion, these findings highlight the significance of aberrant NEDD4L expression in disrupting mitochondrial homeostasis by downregulating CaMKKβ in diabetic kidney disease. This insight offers a potential therapeutic strategy targeting NEDD4L and CaMKKβ to

preserve renal tubular function in the context of diabetes. The potential for therapeutic intervention in this pathway could hold promise for the treatment of DKD.

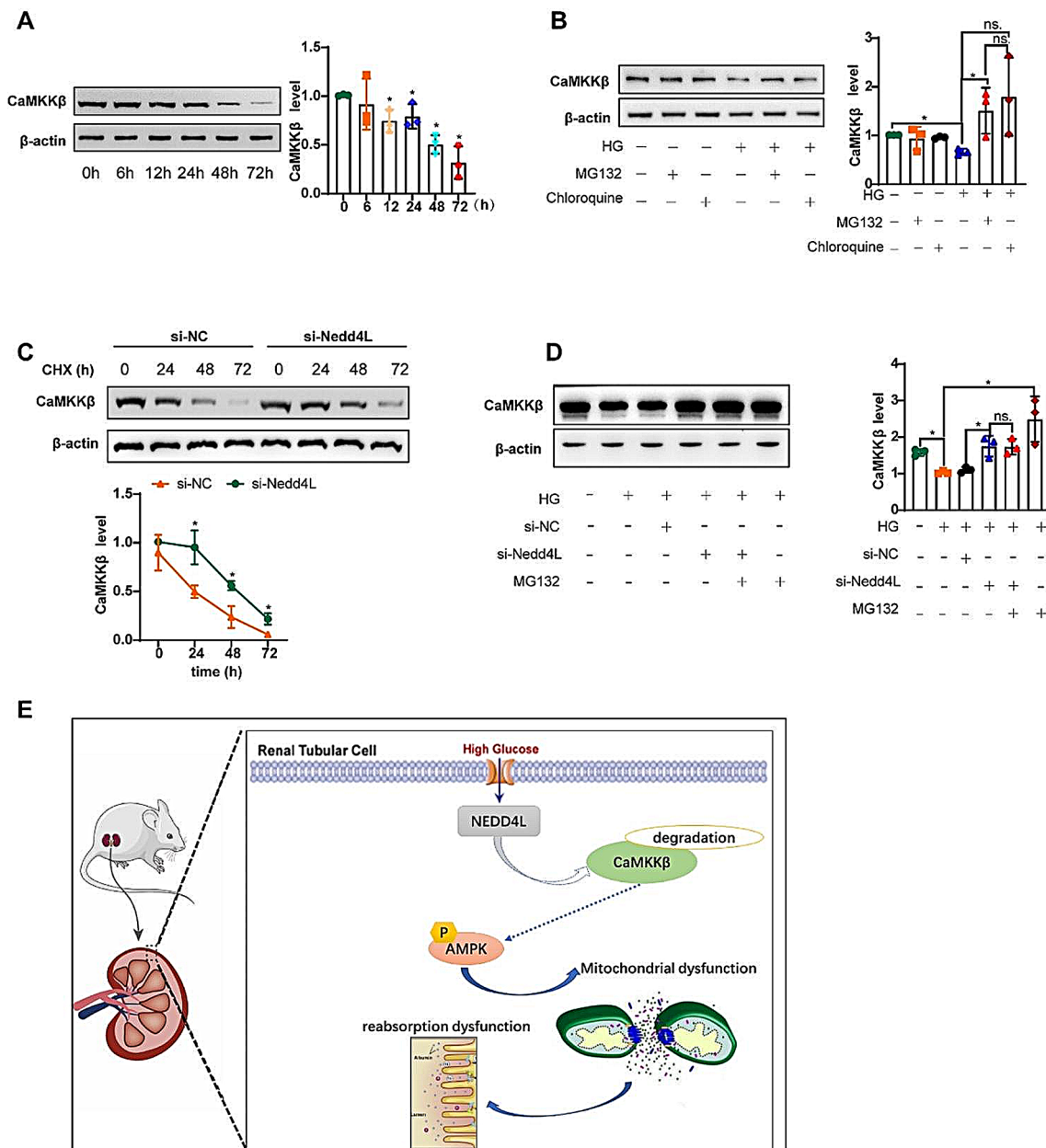


Fig. 8 NEDD4L promotes protein degradation of CaMKKβ. **A** Representative immunoreactive bands for CaMKKβ in HK-2 cells exposed to HG as indicated. **B** Representative immunoreactive bands for CaMKKβ in HK-2 cells treated with 10 μM MG132 or 20 μM chloroquine. **C** HK-2 cells cultured with 25.5mM glucose were transfected with si-NC or si-Nedd4L for 24 h. After coculture with 50 mM cycloheximide (CHX) for 0, 24, 48, or 72 h, western blot analysis was performed, and the relative CaMKKβ expression was calculated. **D** HK-2 cells were transfected with si-NC or si-Nedd4L for 24 h and then treated with or without MG132 for another 48 h. For all the statistical plots, the data are presented as the means ± SEMs. **P* < 0.05; ns. indicates no significance. **E** The expression of NEDD4L was found to be elevated in DKD, leading to the facilitation of CaMKKβ degradation, thereby disrupting mitochondrial homeostasis

Abbreviations

- AAV adeno-associated virus
- AMPK 5' AMP-activated kinase
- BSA bovine serum albumin
- Ca²⁺ calcium ion
- CaMKKβ Calmodulin-dependent protein kinaseβ
- DHE Dihydroethidium
- DKD Diabetic Kidney Disease
- HE Hematoxylin and Eosin
- HG high glucose
- IHC immunohistochemical

- IP immunoprecipitation
- mito-ROS mitochondrial ROS
- PAS Periodic acid-Schiff

Supplementary Information

The online version contains supplementary material available at <https://doi.org/10.1186/s12967-024-05207-6>.

Supplementary Material 1

Acknowledgements

We are grateful to the Bethune Charitable Foundation.

Author Contribution

All the authors contributed to the study conception and design. The experiments, data collection and analysis were performed by Fei Han and Shi Wu. The first draft of the manuscript was written by Fei Han, and all the authors commented on previous versions of the manuscript. Liming Chen designed and conceived this project. Ya Dong and Yanjie Liu analyzed and interpreted the data. Bei Sun supervised the study. All the authors have read and approved the final manuscript.

Funding

This work was supported by the National Natural Science Foundation of China (no. 82370842 and 81900740), the Natural Science Foundation of Tianjin (no. 22JCQNJC01230), the China International Medical Foundation (no. Z-2017-26-2202-2), the Scientific Research Funding of Tianjin Medical University Chu Hsien-I Memorial Hospital [no. ZXY-YJZD2021-1, ZXYZDSYS2022-1], and the Tianjin Key Medical Discipline (Specialty) Construction Project [TJYXZDXK-032 A].

Data availability

The datasets used in the present study are available from the first author upon reasonable request.

Declarations

Ethics approval and consent to participate

The study was conducted in accordance with the guidelines of the Declaration of Helsinki and was approved by the Animal Care Committee of Tianjin Medical University.

Consent for publication

Not applicable.

Competing interests

All the authors declare no competing interests.

Received: 15 February 2024 / Accepted: 15 April 2024

Published online: 16 May 2024

References

1. Souza CS, Deluque AL, Oliveira BM, Maciel ALD, Giovanini C, Boer PA, et al. Vitamin D deficiency contributes to the diabetic kidney disease progression via increase ZEB1/ZEB2 expressions. *Nutr Diabetes*. 2023;13:9.
2. Jefferson JA, Shankland SJ, Pichler RH. Proteinuria in diabetic kidney disease: a mechanistic viewpoint. *Kidney Int*. 2008;74:22–36.
3. Gilbert RE. Proximal Tubulopathy: Prime Mover and Key Therapeutic Target in Diabetic kidney disease. *Diabetes*. 2017;66:791–800.
4. Ho HJ, Aoki N, Wu YJ, Gao MC, Sekine K, Sakurai T et al. A Pacific Oyster-Derived antioxidant, DHMBA, protects Renal tubular HK-2 cells against oxidative stress via reduction of mitochondrial ROS production and fragmentation. *Int J Mol Sci*. 2023; 24.
5. Bhargava P, Schnellmann RG. Mitochondrial energetics in the kidney. *Nat Rev Nephrol*. 2017;13:629–46.
6. Zhou Y, Liu L, Jin B, Wu Y, Xu L, Chang X, et al. Metrnl alleviates lipid Accumulation by modulating mitochondrial homeostasis in Diabetic Nephropathy. *Diabetes*. 2023;72:611–26.
7. Galvan DL, Green NH, Danesh FR. The hallmarks of mitochondrial dysfunction in chronic kidney disease. *Kidney Int*. 2017;92:1051–7.
8. Youle RJ, van der Bliek AM. Mitochondrial fission, fusion, and stress. *Science*. 2012;337:1062–5.
9. Meyer JN, Leuthner TC, Luz AL. Mitochondrial fusion, fission, and mitochondrial toxicity. *Toxicology*. 2017;391:42–53.
10. Su ZD, Li CQ, Wang HW, Zheng MM, Chen QW. Inhibition of DRP1-dependent mitochondrial fission by Mdivi-1 alleviates atherosclerosis through the modulation of M1 polarization. *J Transl Med*. 2023;21:427.
11. Li Q, Liao J, Chen W, Zhang K, Li H, Ma F, et al. NAC alleviates ferroptosis in diabetic nephropathy via maintaining mitochondrial redox homeostasis through activating SIRT3-SOD2/Gpx4 pathway. *Free Radic Biol Med*. 2022;187:158–70.
12. Lee A, Kondapalli C, Virga DM, Lewis TL Jr., Koo SY, Ashok A, et al. Abeta42 oligomers trigger synaptic loss through CAMKK2-AMPK-dependent effectors coordinating mitochondrial fission and mitophagy. *Nat Commun*. 2022;13:4444.
13. Meng M, Li X, Wang Z, Huo R, Ma N, Chang G, et al. A high-concentrate diet induces inflammatory injury via regulating ca(2+)/CaMKKbeta-mediated autophagy in mammary gland tissue of dairy cows. *Front Immunol*. 2023;14:1186170.
14. Yang L, Wang B, Guo F, Huang R, Liang Y, Li L, et al. FFAR4 improves the senescence of tubular epithelial cells by AMPK/Sirt3 signaling in acute kidney injury. *Signal Transduct Target Ther*. 2022;7:384.
15. Sekar P, Hsiao G, Hsu SH, Huang DY, Lin WW, Chan CM. Metformin inhibits methylglyoxal-induced retinal pigment epithelial cell death and retinopathy via AMPK-dependent mechanisms: reversing mitochondrial dysfunction and upregulating glyoxalase 1. *Redox Biol*. 2023;64:102786.
16. Cui T, Wang X, Hu J, Lin T, Hu Z, Guo H, et al. Molybdenum and cadmium co-exposure induces CaMKKbeta/AMPK/mTOR pathway mediated-autophagy by subcellular calcium redistribution in duck renal tubular epithelial cells. *J Inorg Biochem*. 2022;236:111974.
17. Zhou D, Zhou M, Wang Z, Fu Y, Jia M, Wang X, et al. Progranulin alleviates podocyte injury via regulating CAMKK/AMPK-mediated autophagy under diabetic conditions. *J Mol Med (Berl)*. 2019;97:1507–20.
18. Lim JH, Kim HW, Kim MY, Kim TW, Kim EN, Kim Y, et al. Cinacalcet-mediated activation of the CaMKKbeta-LKB1-AMPK pathway attenuates diabetic nephropathy in db/db mice by modulation of apoptosis and autophagy. *Cell Death Dis*. 2018;9:270.
19. Mukherjee R, Das A, Chakrabarti S, Chakrabarti O. Calcium dependent regulation of protein ubiquitination - interplay between E3 ligases and calcium binding proteins. *Biochim Biophys Acta Mol Cell Res*. 2017;1864:1227–35.
20. Yang B, Kumar S, Nedd4 and Nedd4-2: closely related ubiquitin-protein ligases with distinct physiological functions. *Cell Death Differ*. 2010;17:68–77.
21. Lee DE, Yoo JE, Kim J, Kim S, Kim S, Lee H, et al. NEDD4L downregulates autophagy and cell growth by modulating ULK1 and a glutamine transporter. *Cell Death Dis*. 2020;11:38.
22. Xue M, Fang T, Sun H, Cheng Y, Li T, Xu C, et al. PACS-2 attenuates diabetic kidney disease via the enhancement of mitochondria-associated endoplasmic reticulum membrane formation. *Cell Death Dis*. 2021;12:1107.
23. Li P, Zhen Y, Kim C, Liu Z, Hao J, Deng H, et al. Nimbolide targets RNF114 to induce the trapping of PARP1 and synthetic lethality in BRCA-mutated cancer. *Sci Adv*. 2023;9:eadg7752.
24. Zhong Y, Jin R, Luo R, Liu J, Ren L, Zhang Y et al. Diosgenin targets CaMKK2 to Alleviate Type II Diabetic Nephropathy through improving Autophagy, Mitophagy and mitochondrial dynamics. *Nutrients* 2023; 15.
25. Kim K, Lee EY. Excessively enlarged Mitochondria in the kidneys of Diabetic Nephropathy. *Antioxid (Basel)*. 2021; 10.
26. Wang J, Peng Q, Lin Q, Childress C, Carey D, Yang W. Calcium activates Nedd4 E3 ubiquitin ligases by releasing the C2 domain-mediated auto-inhibition. *J Biol Chem*. 2010;285:12279–88.
27. Al-Qusairi L, Basquin D, Roy A, Rajaram RD, Maillard MP, Subramanya AR, et al. Renal tubular ubiquitin-protein ligase NEDD4-2 is required for renal adaptation during long-term potassium depletion. *J Am Soc Nephrol*. 2017;28:2431–42.
28. Wu P, Su XT, Gao ZX, Zhang DD, Duan XP, Xiao Y, et al. Renal tubule Nedd4-2 Deficiency stimulates Kir4.1/Kir5.1 and thiazide-sensitive NaCl cotransporter in Distal Convoluted Tubule. *J Am Soc Nephrol*. 2020;31:1226–42.
29. Jespersen T, Membrez M, Nicolas CS, Pitard B, Staub O, Olesen SP, et al. The KCNQ1 potassium channel is down-regulated by ubiquitylating enzymes of the Nedd4/Nedd4-like family. *Cardiovasc Res*. 2007;74:64–74.
30. Morgenstern TJ, Nirwan N, Hernandez-Ochoa EO, Bibollet H, Choudhury P, Laloudakis YD, et al. Selective posttranslational inhibition of ca(V)beta(1)-associated voltage-dependent calcium channels with a functionalized nanobody. *Nat Commun*. 2022;13:7556.
31. Kim HS, Green YS, Xie Y, Christian JL. Tril dampens nodal signaling through Pellino2- and Traf6-mediated activation of Nedd4I. *Proc Natl Acad Sci U S A*. 2021; 118.
32. Liu S, Guo R, Xu H, Yang J, Luo H, Yeung SJ, et al. 14-3-3sigma-NEDD4L axis promotes ubiquitination and degradation of HIF-1alpha in colorectal cancer. *Cell Rep*. 2023;42:112870.

33. Henshall TL, Manning JA, Alfassy OS, Goel P, Boase NA, Kawabe H, et al. Deletion of Nedd4-2 results in progressive kidney disease in mice. *Cell Death Differ*. 2017;24:2150–60.

Publisher's Note

Springer Nature remains neutral with regard to jurisdictional claims in published maps and institutional affiliations.